Resistance to age-dependent thymic atrophy in long-lived mice that are deficient in pregnancy-associated plasma protein A

Abbe N. Vallejo[a,b,c,d,e,1], Joshua J. Michel[a,c], Laurie K. Bale[f], Bonnie H. Lemster[a,c], Lisa Borghesi[b,d], and Cheryl A. Conover[f]

Departments of [a]Pediatrics and [b]Immunology, [c]Children's Hospital of Pittsburgh, [d]Pittsburgh Cancer Institute, [e]McGowan Institute, University of Pittsburgh, Pittsburgh, PA 15201; and [f]Endocrine Research, Mayo Clinic, Rochester, MN 55905

Edited by Cynthia J. Kenyon, University of California, San Francisco, CA, and approved May 14, 2009 (received for review July 19, 2008)

Pregnancy-associated plasma protein A (PAPPA) is a metalloproteinase that controls the tissue availability of insulin-like growth factor (IGF). Homozygous deletion of *PAPPA* in mice leads to lifespan extension. Since immune function is an important determinant of individual fitness, we examined the natural immune ecology of *PAPPA*$^{-/-}$ mice and their wild-type littermates reared under specific pathogen-free condition with aging. Whereas wild-type mice exhibit classic age-dependent thymic atrophy, 18-month-old *PAPPA*$^{-/-}$ mice maintain discrete thymic cortex and medulla densely populated by CD4^{+}CD8^{+} thymocytes that are capable of differentiating into single-positive CD4 and CD8 T cells. Old *PAPPA*$^{-/-}$ mice have high levels of T cell receptor excision circles, and have bone marrows enriched for subsets of thymus-seeding progenitors. *PAPPA*$^{-/-}$ mice have an overall larger pool of naive T cells, and also exhibit an age-dependent accumulation of CD44^{+}CD43^{+} memory T cells similar to wild-type mice. However, CD43^{+} T cell subsets of old *PAPPA*$^{-/-}$ mice have significantly lower prevalence of 1B11 and S7, glycosylation isoforms known to inhibit T cell activation with normal aging. In bioassays of cell activation, splenic T cells of old *PAPPA*$^{-/-}$ mice have high levels of activation antigens and cytokine production, and also elicit Ig production by autologous B cells at levels equivalent to young wild-type mice. These data suggest an IGF-immune axis of healthy longevity. Controlling the availability of IGF in the thymus by targeted manipulation of PAPPA could be a way to maintain immune homeostasis during postnatal development and aging.

aging | insulin-like growth factor | T cells | thymus

Pregnancy-associated plasma protein A (PAPPA) is a newly recognized zinc metalloproteinase. It degrades inhibitory insulin-like growth factor (IGF)-binding proteins (IGFBP) that limit availability of IGF ligands (IGF1 and IGF2) for IGF receptor (IGFR) signaling (1, 2). Thus, PAPPA is a major regulator of local IGF action.

IGFs are essential for normal fetal and postnatal development. In general, IGF2 is considered the major IGF during early embryogenesis, whereas IGF1 is more important postnatally in rodents. Thus, homozygous mutants of IGF1, IGF2, and IGFR are born dwarfs. However, unlike IGF2 mutants that maintain normal postnatal growth, IGF1 mutants show growth retardation and are short-lived (3, 4). Homozygous IGFR mutation in mice is perinatal lethal (4), but IGFR heterozygotes are viable and live longer than wild-type mice (5). On the other hand, young transgenic IGF1 and IGF2 mice exhibit organomegaly (6, 7), and IGF1 is also associated with vascular inflammation, and tumor growth and metastasis in adults (8, 9).

The basis for these seeming antagonistic effects of IGF is a subject of significant interest (10, 11), but has been difficult to elucidate due to the complexity of the IGF system and limitations in available models (12, 13). IGF1 and IGFR mutant mice are not viable. Ames and Snell mice, 2 models of longevity, have deficiency in circulating IGF1 as a result of primary mutations in growth hormone (GH) synthesis pathway that regulates liver-derived IGF1 (14). They also have deficiencies in many pituitary hormones and are prone to metabolic disorders that lead to age-related morbidity. So teasing out specific effects of IGF from GH on the biology of longevity using Ames and Snell mice has been technically challenging.

We generated *PAPPA*$^{-/-}$ mice (15) to test the hypothesis that control of the tissue availability, independent from systemic levels, of IGF influences development and the aging process. We reported that *PAPPA*$^{-/-}$ mice develop normally and are fertile (15). They are proportional dwarfs; their organs smaller than wild-type littermates, without signs of loss/enlargement of particular organs. They survive well in specific pathogen-free (SPF) vivarium. Akin to *C. elegans* and *Drosophila* where mutation or attenuation of the expression of molecules of the homologous IGF signaling pathway extend lifespan (10–14), *PAPPA*$^{-/-}$ mice have prolonged survival. Compared with their wild-type littermates, they have lifespan extension of 33% and 41% for males and females, respectively (16). Levels of IGF1 in circulation and in various non-lymphoid tissues are equivalent to that seen in wild-type mice, but levels of available bioactive IGF for IGFR signaling is lower for *PAPPA*$^{-/-}$ mice (15, 17, 18). Their metabolic rate, and serum levels of glucose, insulin, cholesterol, and GH are also equivalent to those of wild-type mice (15, 16, 19). Hence, longevity of PAPPA$^{-/-}$ mice is unlikely to be due to metabolic or circulating IGF/GH abnormalities.

PAPPA$^{-/-}$ mice also have significantly reduced burden of tumors compared with their wild-type littermates (16). Necropsy of old *PAPPA*$^{-/-}$ mice that died shows sporadic occurrence of small-size tumors of a single type. In contrast, necropsy of dead wild-type mice shows large multiple tumors in liver, lung, kidney, and colon, along with splenomegaly and lymphomegaly. The basis for this observation is unknown. However, because immune function is vital to individual health and survival (20, 21), we hypothesized that maintenance of immune homeostasis might underlie the apparent healthy longevity of *PAPPA*$^{-/-}$ mice. This hypothesis is based on reports that IGF1 and IGF2 are required for early organogenesis such as for muscle and thymus, yet infusion of recombinant IGF1 in old mice neither prevents muscle wasting nor reconstitutes the involuted aged thymus (22–24).

In this study, we assessed age-related immunological changes in *PAPPA*$^{-/-}$ and wild-type mice raised in SPF vivarium. Since SPF is not a germ-free sterile environment, we were able to monitor the normal immune ecology of the animals analogous to the environmental situation of feral mice and humans.

Results

Moribund animals, mostly old wild-type mice with high tumor burden (16), were excluded. Mice were euthanized, and lymphoid

Part of this work was presented in abstract form at the 96th Annual Meeting of the American Association of Immunologists, Seattle, WA, May 8–12, 2009.

Author contributions: A.N.V. designed research; A.N.V., J.J.M., L.K.B., B.H.L., L.B., and C.A.C. performed research; L.K.B. and C.A.C. contributed new reagents/analytic tools; A.N.V. and J.J.M. analyzed data; and A.N.V. wrote the paper.

The authors declare no conflict of interest.

This article is a PNAS Direct Submission.

Freely available online through the PNAS open access option.

[1]Address correspondence to Abbe N. de Vallejo. E-mail: andv26@pitt.edu.

www.pnas.org/cgi/doi/10.1073/pnas.0807025106

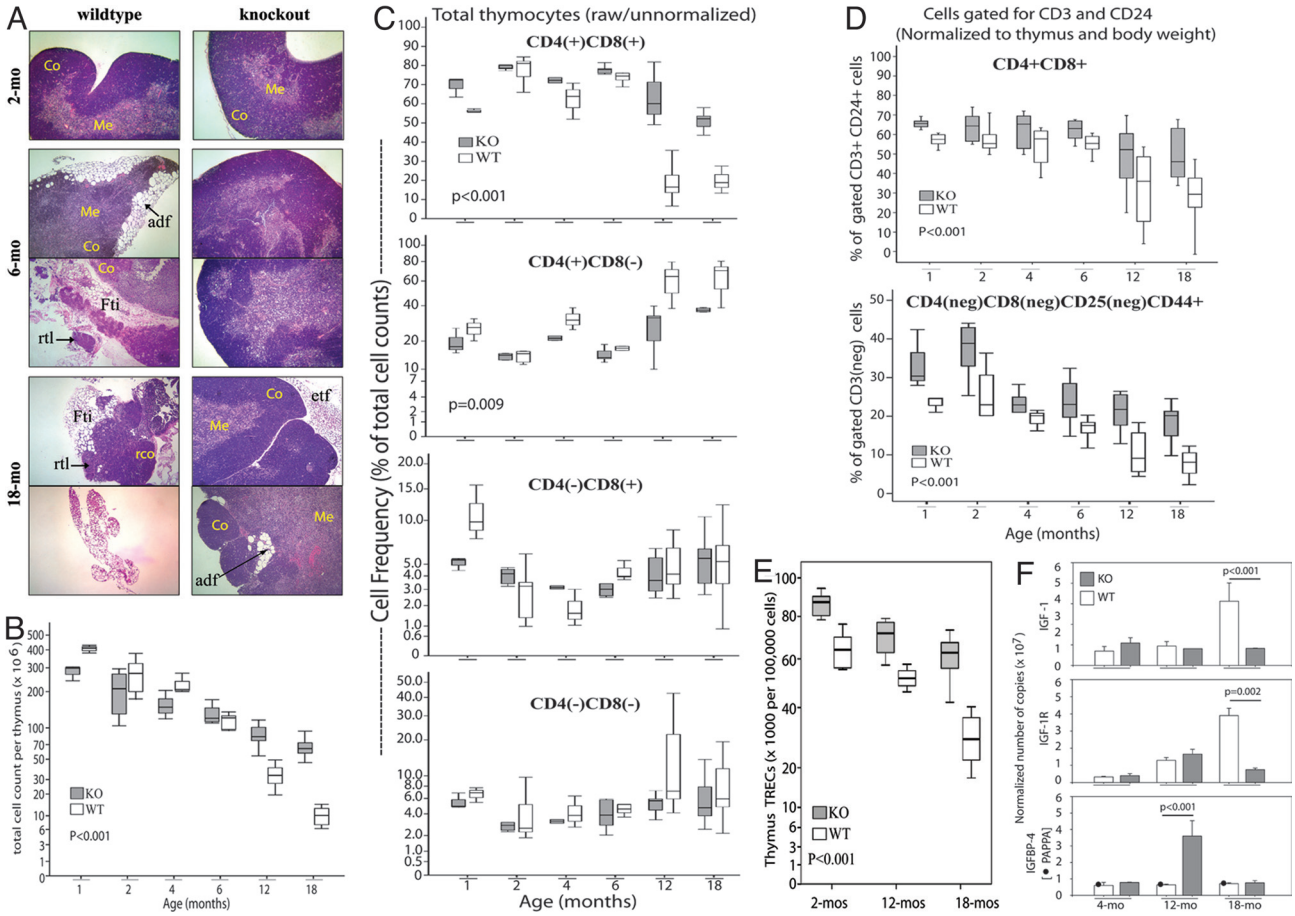

Fig. 1. *PAPPA*$^{-/-}$ mice are resistant to thymic atrophy with aging. (*A*) Frozen sections of wild-type (*WT*) and *PAPPA*$^{-/-}$ (KO or knockout) thymi were stained with H&E and analyzed by microscopy. (Magnification: 20×.) Micrographs shown were representative of 5–7 thymi per group, at 3 consecutive sections per thymus. Co, cortex; Me, medulla; adf, adipocyte infiltrate; etf, extrathymic fat tissue; Fti, intrathymic fat; rco, residual thymic cortex; rtl, residual thymic lobe. (*B*) Thymocyte suspensions (n = 5–12 mice per group) were counted. Data shown are box/whisker plots of raw cell counts. Boxes mark the 25th and 75th percentile values; the line inside each box is the median; and whiskers indicate the spread of 5th and 95th percentiles; the *P* value was determined by ANOVA. (*C*) Thymocyte suspensions were analyzed by flow cytometry. Box/whisker plots (10–17 mice per group) shown are the raw percentages of cells expressing CD4, or CD8 or both, without gating for CD3 or CD24. (*D*) The cytometry data set in *C* were reanalyzed by gating for CD3 and CD24, and then for the expression of CD4, CD8, and CD25. Data shown are box/whisker plots of $CD3^+CD24^+$, DP cells (*Upper*), and of the immature DN1 thymocytes defined as $CD3^-CD4^-CD8^-CD24^+CD25^-CD44^+$ (*Lower*). Data were normalized for thymus and body weight. Box/whisker plots (and *P* values) in *C* and *D* were determined as in *B*. (*E*) Thymic TREC levels (7 mice per group) were measured by quantitative PCR. Box/whisker plots from 100,000 cells (and *P* value) were determined as in *B*. (*F*) Whole thymi (3–5 per group) were examined for levels of IGF, IGFR, and IGFBP4 transcripts by quantitative RT-PCR. Level of PAPPA in wild-type mice was also measured; the correct size transcript was undetected in *PAPPA*$^{-/-}$ mice as expected. Bar graphs are means (±SEM) normalized to ribosomal L19 transcript. *P* values of the indicated group comparisons were determined by Mann–Whitney *U* test.

tissues and bone marrows were collected. Analysis of lymphoid tissue was limited to thymus and spleen because of low harvest of lymph nodes that were so tiny in *PAPPA*$^{-/-}$ mice due to proportional dwarfism (15).

***PAPPA*$^{-/-}$ Mice Maintain Thymic Structure with Aging.** Thymic atrophy is a signature of aging (25). Histological analysis was therefore done on cryostat sections of thymi stained with hematoxylin/eosin (H&E). Fig. 1*A* shows progressive collapse of thymic structure with age in wild-type mice. There was adipose infiltration of the thymic cortex within 6 months of age. In some mice, adipose infiltration was so extensive that segments of thymic lobes lacked cortex and medulla. At 18 months, most wild-type thymi were very small in size, and histologically resembled fatty tissue, with exceedingly small number of thymocytes. For some 18-month-old wild-type thymi, there was residual thymic tissue with H&E staining pattern indicating few foci of cortical thymocytes. Box/whisker plots in Fig. 1*B* show that age-dependent thymic atrophy corresponded with progressive decreases in thymus cellularity.

In contrast, *PAPPA*$^{-/-}$ mice maintained discrete cortex and medulla with aging, indicated by differential high-intensity blue and pink H&E staining, respectively (Fig. 1*A*). There was dense cellularity of *PAPPA*$^{-/-}$ thymi even at 18 months of age. Fat tissues were recovered with some old *PAPPA*$^{-/-}$ thymi, but they were extrathymic. Some 18-month-old *PAPPA*$^{-/-}$ thymi had sporadic small adipose foci within the cortex, but the overall thymic architecture was maintained.

Maintenance of thymic structure corresponded with overall high degree of cellularity into old age. Fig. 1*B* shows that young *PAPPA*$^{-/-}$ thymi had lower absolute cell numbers consistent with dwarfism, but thymi of 12–18-month-old *PAPPA*$^{-/-}$ mice contained significantly higher cell numbers than old wild-type thymi ($P < 0.001$). Normal thymus histology, and overall preservation of thymocyte numbers, correlated with significantly larger thymic volume, corrected for body size, through life among *PAPPA*$^{-/-}$ mice.

Old *PAPPA*$^{-/-}$ Thymi Contain a Large Pool of Immature Thymocytes. We quantified thymocyte subsets by flow cytometry, and present both raw data and data normalized to thymus and body weight. Fig. 1*C* shows that the raw proportion of double-positive (DP) $CD4^+$

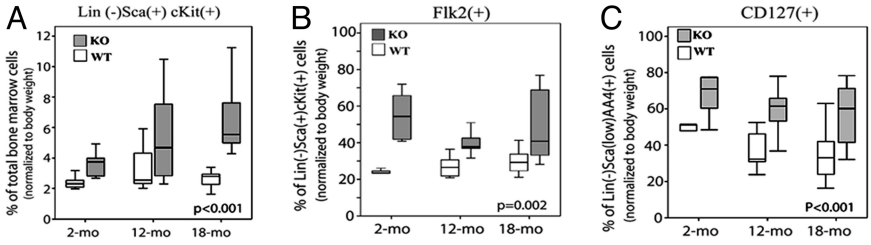

Fig. 2. Old *PAPPA*$^{-/-}$ mice have large pools of thymus-seeding progenitors. Bone marrow aspirates were analyzed by flow cytometry. Box/whisker plots (5–9 mice per group) of (*A*) the most undifferentiated Lin^{-}ScaI^{+}cKit^{+} cells; (*B*) Lin^{-}ScaI^{+}cKit^{+} Flk2^{+} subset that contain lymphoid-primed progenitors; and (*C*) the common lymphoid progenitors Lin^{-}ScaI^{low}AA4^{+}CD127^{+}cells were cell frequencies normalized to body weight. Box/whisker plots (the *P* values) were determined as in Fig. 1*B*.

CD8^{+} thymocytes was higher for *PAPPA*$^{-/-}$ mice than wild-type mice. When cell phenotypes were gated for CD3 and CD24, and normalized to thymus and body weight, Fig. 1*D* (*Top*) shows *PAPPA*$^{-/-}$ mice still showed higher proportions of immature DP CD3^{+} cells ($P < 0.001$), the immediate precursor of single-positive (SP) CD4 and SP CD8 T cells that ultimately seed secondary lymphoid organs (26). Despite individual variation, shown by the spread of DP cell frequency whiskers from the box plot/median, wild-type mice had lower level of DP cells at 12 and 18 months ($P < 0.01$); more than half of them carried <40% DP cells, with combined median of 35%. Their age-matched old *PAPPA*$^{-/-}$ counterparts had narrower spread of DP cell frequency with a higher combined median of 52%.

Thymi of both mice strains contained SP CD4^{+} thymocytes 4–8 times higher than SP CD8^{+} thymocytes; older mice tended to have higher levels of SP cells than younger mice (Fig. 1*C*). The basis for the more dominant development of SP CD4 cells is unknown.

Overall proportion of ungated double-negative (DN) thymocytes was very similar between the 2 strains (Fig. 1*C*). By gating for the expression of CD3, CD25, and CD44, we were able to discriminate the most immature DN subset of T cell precursors (also called "DN1" cells; 26) CD3^{-}CD4^{-}CD8^{-}CD25^{-}CD44^{+} cells. Data in Fig. 1*D* (*Lower*) show that *PAPPA*$^{-/-}$ mice had overall higher proportion of DN1 cells ($P < 0.001$). Relative to their larger body size, 12- or 18-month-old wild-type mice had lower levels of DN1 cells with combined median frequency of 10%, compared with 22% for 18-month-old *PAPPA*$^{-/-}$ mice.

Old *PAPPA*$^{-/-}$ Thymi Actively Produce New T Cells. Old *PAPPA*$^{-/-}$ thymi were examined for the production of new T cells by quantitative PCR measurements of T cell receptor (TCR) excision circles (TREC), episomal DNA excised during *TCR A* gene rearrangement after the DN1 stage of thymocyte differentiation (26, 27). Fig. 1*E* shows that *PAPPA*$^{-/-}$ mice had overall higher TREC levels ($P < 0.001$). Wild-type mice had median 28,000 TREC/100,000 cells at 18 months, an ≈60% reduction from median 65,000 TREC at 2 months. In contrast, *PAPPA*$^{-/-}$ mice had a median 84,000 and 62,000 TREC at 2 and 18 months, respectively; an ≈30% reduction with age, but old *PAPPA*$^{-/-}$ thymi still had high TREC level equivalent to young wild-type mice.

Old *PAPPA*$^{-/-}$ Thymi Express Lower Steady-state Levels of IGF1. The above thymic properties correlated with thymic IGF1 expression. Results of RT-PCR assays in Fig. 1*F* shows that wild-type, but not *PAPPA*$^{-/-}$, mice had age-dependent increases in thymic IGFR and IGF1. At 18 months, wild-type thymi had higher IGFR/IGF1 levels than *PAPPA*$^{-/-}$ thymi ($P < 0.001$). In contrast, IGFBP4, the major PAPPA substrate, was higher in 12-month-old *PAPPA*$^{-/-}$ thymi ($P < 0.001$). Similar PCR assays with spleen, kidney, and liver did not show differences in IGFR/IGF1 transcript levels between age-groups and genotype, consistent with our previous studies (15–19). All these data suggest increased thymus-specific IGF signaling with normal aging that could exhaust the pool of immature thymocytes; increased IGFBP4 levels in old *PAPPA*$^{-/-}$ thymi could attenuate IGF signaling and prolong thymopoiesis.

Old *PAPPA*$^{-/-}$ Bone Marrow Retain Thymus-Seeding Progenitor Subsets. Thymopoiesis depends on the supply of progenitors from the bone marrow, hence hematopoietic cells of wild-type and *PAPPA*$^{-/-}$ mice were examined. Fig. 2*A* shows age-related increased frequency of lin^{-}ScaI^{+}cKit^{+} (or LSK) cells, the most undifferentiated subset of bone marrow cells (28). Fig. 2 *B* and *C* show age-related decreased frequency of 2 subsets that contain lymphoid-primed progenitors; the Flk2^{+} LSK cells, and the more advanced common lymphoid progenitor CD127^{+}lin^{-}ScaI^{low}AA4^{+} cells (28). However, *PAPPA*$^{-/-}$ mice had overall significantly higher proportions of these 3 progenitor subsets compared with wild type. Whether survival and multipotential properties of these progenitors are prolonged by *PAPPA* deletion remains to be examined. These data are consistent with DP/DN1 thymocyte frequencies (Fig. 1), indicating that old *PAPPA*$^{-/-}$ mice maintain cell precursor pools in both bone marrow and thymus from which naive T cells are ultimately derived.

All of the above data are consistent with reports about a role of the IGF system in thymopoiesis. High thymic IGF levels are found fetal thymi (23). Thymic organ cultures treated with antibodies to IGF1, IGF2, or IGFR show arrested development of DP thymocytes (29). Young IGF transgenic mice have hypercellular thymi and generalized organomegaly (6, 7, 30), but develop multiple tumors leading to early mortality (6, 9). IGFBP4 transgenic mice have impaired thymus organogenesis (31). The physiological impact of transgenic IGF1, IGF2, and IGFBP4 in old age has not been examined. *IGFBP4*$^{-/-}$ mice are 85–90% smaller than wild-type mice (32), but are still considerably larger than dwarf *PAPPA*$^{-/-}$ mice (15). Whether or not *IGFBP4*$^{-/-}$ mice have similar lifespan and immunological properties as *PAPPA*$^{-/-}$ mice needs to be examined.

Old *PAPPA*$^{-/-}$ Mice Have Indicators of Active Seeding of the Peripheral T cell Compartment. Fig. 3*A* shows that DP CD3^{+} cells from old and young *PAPPA*$^{-/-}$ thymi developed into SP CD4, and SP CD8, CD3^{+} T cells after stimulation with anti-CD3 as efficiently as similar DP cells from young wild-type mice. In all thymi examined, SP CD4 cells were always higher than SP CD8 cells even when DP were coactivated with anti-CD8. And consistent with the proapoptotic effect of CD28 costimulation for normal mouse thymocytes (33), we also found that incubation of DP cells of both *PAPPA*$^{-/-}$ and wild-type mice with anti-CD3 and anti-CD28 resulted in massive cell death. All of these observations indicate that DP cells in old *PAPPA*$^{-/-}$ thymi constitute a pool of viable, immature precursors rather than a pool of developmentally defective thymocytes.

Fig. 3*B* shows the results of TREC analysis of splenic T cells as indicator of recent T cell emigrants from the thymus (27). Both mice strains showed an age-dependent decline splenic TREC, similar to that of thymic TREC (Fig. 1*E*). However, *PAPPA*$^{-/-}$ spleens had an overall higher TREC than wild-type spleens ($P < 0.001$). At 18 months, wild-type splenic TREC levels were exceedingly low, 120 TREC/100,000 cells. In contrast, 18-month *PAPPA*$^{-/-}$ spleens had a median 2,000 TREC.

***PAPPA*$^{-/-}$ Mice Have Robust Naive and Memory T cell Compartment.** Flow cytometry showed that old *PAPPA*$^{-/-}$ spleens contain large pool of naive T cells. Fig. 3*C* shows age-related contraction in the

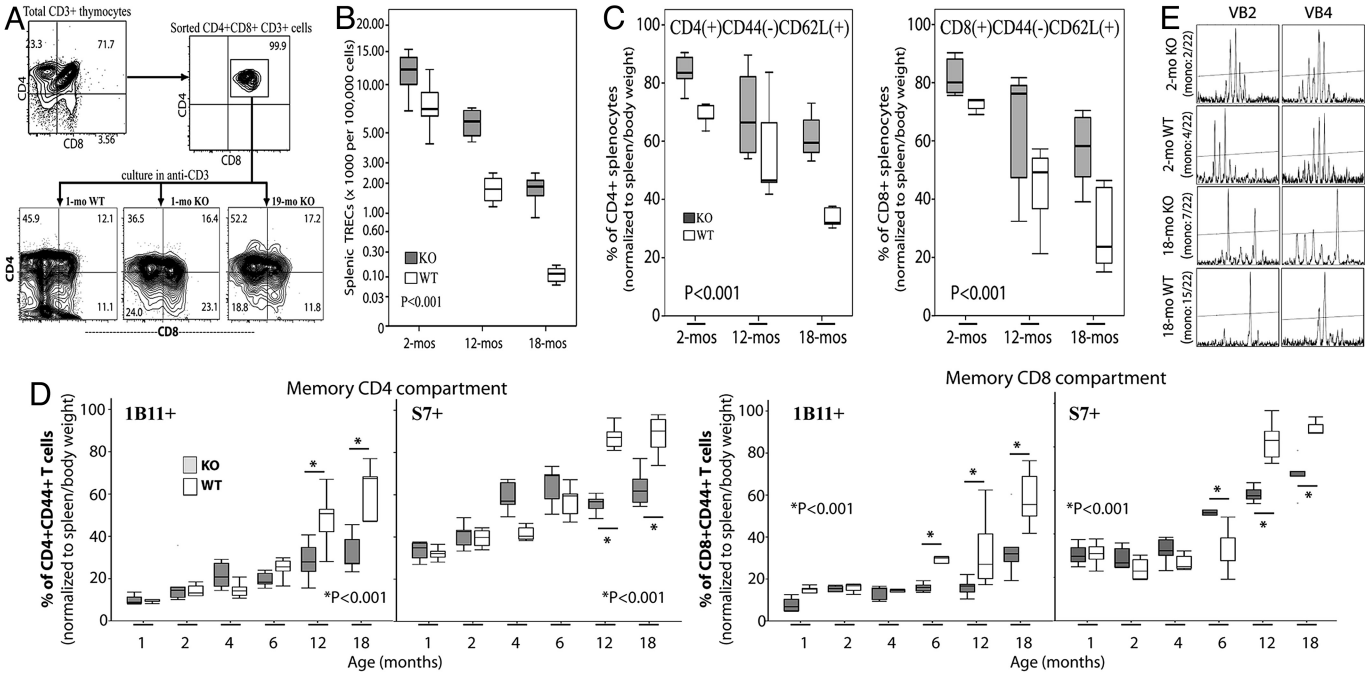

Fig. 3. Old *PAPPA*$^{-/-}$ mice have robust peripheral T cell repertoire. (*A*) DP cells of 1-month-old wild-type (WT), and 1-/19-month-old *PAPPA*$^{-/-}$ (KO) thymi were isolated by cell sorting; incubated in plate-immobilized anti-CD3; and analyzed for CD3, CD4, and CD8 expression after 3 days by flow cytometry. Data shown were representative of 5 mice per age-group examined. (*B*) Spleens were collected. Splenic TREC levels per 100,000 cells from 5–7 mice per group were measured as in Fig. 1*E*. (*C*) Splenocytes were analyzed by flow cytometry for the frequencies of naive CD4 and CD8 T cells defined as CD44^{-}CD62L^{+} (5–9 mice per group). (*D*) Cytometric analysis of memory cells defined as CD44^{+}S7^{+}(1B11^{+}) CD4 and CD8 T cells was also done (6–9 mice per group). Asterisk (*) denote significant difference ($P < 0.001$; Mann–Whitney) between the 2 indicated groups. Box/whisker plots (and *P* values) in *B–D* were determined as in Fig. 1*B*; plots in *C* and *D* were normalized to spleen and body weights. (*E*) T cells were isolated from spleens (3 mice per group) by cell sorting, and subjected to *CDR3* spectratyping of 22 *TCR BV*. Data shown were representative VB2/VB4 spectratypes illustrating Poisson distribution of *CDR3* lengths in young mice. Poisson spectratypes, indicating high VB diversity, were infrequent in old mice as shown by limited number of CDR3 signal peaks. Mono, average occurrence of monoclonal, single-peak *CDR3* spectratype.

sizes of the naive CD4 and CD8 T cell compartments in both mice strains. However, *PAPPA*$^{-/-}$ mice had an overall higher pool of CD4 and CD8 naive CD44^{neg}CD62L^{+} CD3^{+} splenocytes ($P <$ 0.001). Whereas 18-month-old wild-type mice had a combined naive CD4 and CD8 median of ≈30% CD44^{neg}CD62L^{+} splenocytes, the combined naive compartment of 18-month *PAPPA*$^{-/-}$ mice was ≈60% CD44^{neg}CD62L^{+} splenocytes.

Aging is associated with the increase in memory T cells (21), a phenomenon attributed to impaired T cell production (Fig. 1*E*), and to depletion of naive T cells (Fig. 3*C*) that become transformed into memory cells due to antigenic exposure through life (21, 34). Hence, we examined whether maintenance of the thymus in *PAPPA*$^{-/-}$ mice (Fig. 1*A*) alters formation of the memory compartment. Cytometry data in Fig. 3*D* shows the progressive accumulation of memory CD44^{+}CD43^{+} CD4 and CD8 T cells with aging in both mice strains. An important difference is that 12- and 18-month-old *PAPPA*$^{-/-}$ mice had lower levels of CD43^{+} T cells than age-matched wild-type mice. The 2 glycosylation forms of CD43, 1B11 and S7, which had been reported to inhibit CD3-mediated activation of T cells (35), were significantly higher in the wild type.

Old *PAPPA*$^{-/-}$ Mice Have a Diverse TCR Repertoire. Size contraction of the naive reserve with aging has been attributed to monoclonal expansion of T cells that effectively contract the overall diversity of the TCR repertoire (21, 36). Hence, spectratype analysis of the *CDR3* segment of 22 TCR β chains was done to examine whether old *PAPPA*$^{-/-}$ mice had robust T cell repertoire. Fig. 3*E* shows representative *CDR3* spectratypes; that is, ladders of PCR amplification products of *BV-BJ* junctions of recombined *TCR BV* with multiple signal peaks indicating polyclonal diversity for the given *CDR3* segment. As expected, there was Poisson distribution of multiple *CDR3* segments in young mice of both strains; whereas old mice had reduced numbers of *CDR3* segments. For example, there was an average of only 2 and 4 TCR VB2 and VB4 spectratypes that had a single, or monoclonal, *CDR3* peak in 2-month-old wild-type and *PAPPA*$^{-/-}$ mice, respectively. At 18 months, wild-type mice had an average of 15 monoclonal VB2/VB4 spectratypes. In contrast, spectratypes of old *PAPPA*$^{-/-}$ mice generally had higher numbers of signal peaks, with an average 7 monoclonal VB2/VB4 spectratypes, or only 30% reduction of VB2/VB4 diversity compared with 60% in wild-type mice ($P < 0.05$).

T Cells of Old *PAPPA*$^{-/-}$ Mice Respond to Classical Activating Stimuli. Relevance of maintaining the thymus with aging ultimately depends on whether the T cells of old mice are functional. Thus, cellular bioassays were performed by incubating splenocytes of young and old mice with anti-CD3 and anti-CD28, a strategy that specifically activates T cells (37). Since the impact of *PAPPA* deletion on function of other immune cells, that is, B cells, dendritic cells; have yet to be ascertained; and that normal aging has been shown to alter immune cell numbers that differentially influence immune outcomes (38–40), we used unfractionated splenocytes to assess T cell activation in the midst of all of the other cells, depletion of any 1 cell type could adversely affect experimental outcomes.

Fig. 4*A* shows CD3/CD28-mediated activation of splenic T cells of old *PAPPA*$^{-/-}$ mice as efficiently as for young wild-type and *PAPPA*$^{-/-}$ mice. There were equivalent levels of CD25 and CD69; and also nearly identical levels of Ki67, a molecular marker for the movement of quiescent cells into the active phases of cell cycle (41), in both CD4 and CD8 subsets. Old wild-type splenocytes incubated in anti-CD3/CD28 showed negligible expression of these molecules.

Activation of T Cells of Old *PAPPA*$^{-/-}$ Mice Leads to Cytokine and Ig Production. Fig. 4*B* shows anti-CD3/CD28-induced up-regulation of the T-helper antigen CD154 on CD4 T cells, with corresponding

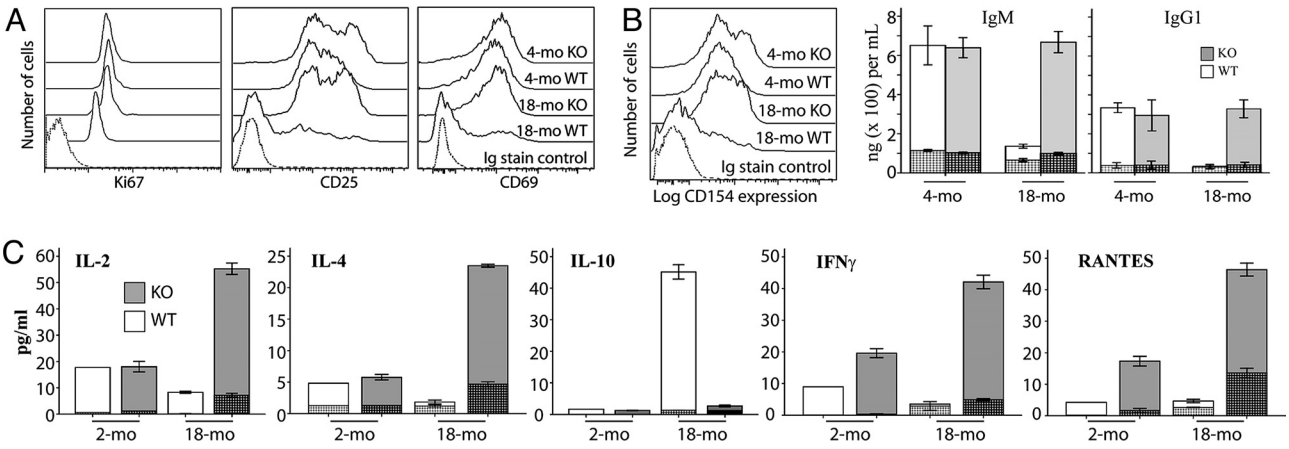

Fig. 4. Mature T cells of old *PAPPA*$^{-/-}$ mice are functional. Splenocytes from 2-/18-month-old wild-type (WT) and *PAPPA*$^{-/-}$ (KO) mice (7 per group) were stimulated with anti-CD3 and anti-CD28, or IgG control; cells and supernatants harvested after 5 days. (*A*) T cell phenotypes were examined by flow cytometry. Histograms shown were representative profiles of CD3/CD28-stimulated cells for the expression of Ki67, CD25, and CD69 in electronically gated CD3^{+}CD4^{+} T cells. Control cultures, irrespective of genotype and age, incubated in IgG had expression profiles that were superimposable with histogram of IgG isotype staining controls. Similar expression levels for these molecules were seen for CD3^{+} CD8^{+} T cells. (*B*) Expression of the T helper antigen CD154 was also examined by flow cytometry. IgG/IgM production in the culture supernatants was measured by ELISA. (*C*) Cytokine content of the supernatants was measured by the Luminex system. Tall white and gray bar graphs (5 mice per group) in *B* and *C* are weighted means of triplicate measurements (± SEM) of CD3/CD28-stimulated cells. Hatched bars inside the tall bar graphs were measurements from control cells incubated in IgG.

high levels of IgM and IgG in the culture supernatants. These data suggest productive interaction between activated CD4 T cells and B cells in culture.

CD3/CD28-mediated activation of T cells also resulted in higher levels of production of cytokines in old *PAPPA*$^{-/-}$ mice compared with young wild-type or young *PAPPA*$^{-/-}$ mice ($P < 0.05$). Of 21 molecules examined, IL-2, IL-4, IFN-γ, RANTES (Fig. 4*C*), IL-12p70, and CCL4/MIP-β were produced by activated cells of old *PAPPA*$^{-/-}$ mice at ≥3 times the levels of production by similar cells of young mice. In contrast, splenocytes of old wild-type mice incubated in anti-CD3/CD28 did not show substantial expression levels of activation antigens or cytokine/Ig production over IgG-incubated cells, consistent with various reports about malfunctions of T cells from normal aged mice (38). However, old wild-type, but not *PAPPA*$^{-/-}$, mice showed CD3/CD28-mediated induction of IL-10 (Fig. 4*C*), an attenuator of CD3-driven T cell activation. Similar results were obtained with splenic cultures incubated in the mitogen Con A. All these data indicate overall functional competence of T cells in old *PAPPA*$^{-/-}$ mice. We are accruing stocks of *PAPPA*$^{-/-}$ mice older than 24 months for antigen challenge studies to investigate if their longevity is linked to maintenance of adaptive immunity.

Discussion

Long-lived *PAPPA*$^{-/-}$ mice, in contrast to wild-type mice, resist age-dependent thymic atrophy (Fig. 1) and maintain a pool of functionally competent T cells in their old age (Fig. 4). PAPPA$^{-/-}$ mice are a distinctive mammalian model of healthy longevity, wherein lifespan regulation is GH-independent. Their immune properties are consistent with paradigms about IGF-immune interactions in physiological homeostasis (8, 42), and for a central role of immune competence in healthy aging (20, 21).

IGF1 is an inducer of cell proliferation and differentiation including for resident cells in the thymus (29–32). In line with PAPPA's role as regulator of IGF bioavailability (2), intact thymi in old *PAPPA*$^{-/-}$ mice is associated with steady-state level of thymic IGF1 (Fig. 1*F*). Without PAPPA, thymic IGF1 could be more slowly released by other IGFBP proteases that have lesser IGFBP-specificity than PAPPA (43). Slower release of thymic IGF1 could be prolonging the survival of resident thymocyte precursors, and so *PAPPA*$^{-/-}$ mice maintain thymic structure through life. This suggestion is consistent with reports that recombinant IGF1 alone does not fully reconstitute the involuted mouse thymus (24). It will therefore be of interest to examine how PAPPA-dependent restriction of IGF1 availability influences the quality of IGF signaling and effectively controls the rate of proliferation and differentiation of thymocyte progenitors.

Although direct assessment of immune protection against pathogens in old long-lived PAPPA$^{-/-}$ mice has yet to be done, normal development of memory T cells and a pool of diverse and functionally active T cells suggest immune competence in their old age. It is noteworthy that IGF signaling has both positive and negative immune outcomes; that is, IGF1 augments IL-2 production, but inhibits T-helper differentiation and promote tumor growth (9, 44, 45). In line with the idea for the control of IGF bioavailability, reduced tumor burden observed in old *PAPPA*$^{-/-}$ mice (16) could be an outcome of attenuated IGF signaling that effectively fine tunes IGF-mediated immune effector functions. Thus, it will be of interest to examine the extent to which *PAPPA* deletion might directly dampen IGF-induced oncogenic pathways and favor IGF-mediated immune pathways.

Methods

Mice and Collection of Biological Specimens. This study was conducted according to IACUC-approved protocols at Mayo Clinic and University of Pittsburgh. *PAPPA*$^{-/-}$ mice and their wild-type littermates are mixed C57BL/6–129SV/E background; generation and breeding of these strains were described in ref. 15. All mice were maintained with unlimited access to food and water in SPF vivarium. At the indicated age, mice were euthanized; and thymi, spleens, and bone marrows were collected.

Histological Analysis. Thymi were embedded in OCT (TissueTek). Cryostat serial sections of 5-μm-thickness were cut, and processed for standard H&E staining. Slides were examined in blinded fashion using the Diaphot 300 microscope (Nikon) interfaced with automated image capture and analysis with the MetaMorph software (Molecular Devices). At least 3 consecutive sections for each thymus sample were examined.

Flow Cytometry. Single-cell suspensions of thymi or spleen or bone marrow aspirates, or cultures of splenocytes, were examined by multicolor flow cytometry (46). Cells were identified by immunostaining with appropriate fluorochrome-conjugated antibodies (BD; Ebioscience) to classical T cell markers CD3, CD4, and CD8; thymocyte maturation markers CD24, CD44, and CD25; memory markers CD44, S7, and 11B1; naive marker CD62L; bone marrow antigens ScaI, cKit, Flk2,

AA4, and CD127; and lineage (lin) markers (28). For splenic T cell cultures, cell staining included antibodies to CD25, CD69, CD154, and Ki67.

Cytometry experiments included fluorochrome-conjugated beads (Spherotec) for instrument calibration and for off-line signal compensation. Controls were cells singly-stained with reference antibodies for each fluorochrome; cells incubated with IgG isotypes, and unstained cells. Cytometric data were acquired using the LSRII cytometer (BD). Cell populations were by FlowJo software (Tree Star). Live cells were electronically gated from forward and side scatter. Single cells were discriminated by height-vs.-width plot of the forward scatter. Background fluorescence and flourochrome-specific signals were normalized from a compensation matrix constructed from cytometric data of unstained cells, cells incubated in IgG isotypes, and single-stain cells. Because of proportional dwarfism of *PAPPA*$^{-/-}$ mice (15) wherein total cell counts of thymi, spleen, and bone marrow (except for 12- and 18-month-old thymi) were always lower than wild-type mice, cell population data were normalized to body weight and to either thymus or spleen weight as appropriate.

Molecular Assays. Determination of thymic and splenic TREC levels by quantitative PCR was carried out according to previous procedures (27) using the MX3000 QPCR system (Stratagene). Quantitative RT-PCR assays for IGF, IGFR, IGFBP4, and PAPPA were also done according to previous procedures (18) using the iCycler sytem (Bio-Rad). *TCR VB CDR3* spectratyping was performed using TCRExpress kit and software (Biomed Immunotech) following manufacturer specifications.

Thymocyte Differentiation. DP CD4^{+}CD8^{+}, CD3^{+} thymocytes were isolated by standard fluorescence-activated cell sorting using the Aria cytometer (BD), with verified purity of ≥99%. Using published procedures for thymocyte differentiation (33), 1×10^6 DP cells were incubated in plate-immobilized rat anti-mouse CD3 (5 μg/mL) in combination with the same amount of rat anti-mouse CD4 or CD8 or CD28; or in rat IgG alone (all from BD) for 3–5 days. Cell phenotypes were analyzed by flow cytometry.

Splenic T Cell Activation. Bioassays were conducted according to standard procedures (37). Splenocytes (1×10^6 cells per well) were incubated with 10 μg/mL soluble rat anti-mouse CD3 and rat anti-mouse CD28 or rat IgG (all from BD); or with 1 ng/mL Con A (Sigma Aldrich) for 3–5 days. T cell phenotypes, along with the expression of CD25, CD69, CD154, and Ki67, were examined by flow cytometry. Culture supernatants were analyzed for cytokine content using the Luminex system with Bioplex kit (Bio-Rad) following previous procedures (46) using mouse-specific cytokine standards. Levels of IgM and IgG in the supernatants were measured by quantitative ELISA using commercial kits (Bethyl Labs).

Statistical Analysis. Quantitative data were analyzed non-parametrically using SPSS software (SPSS Inc.). Phenotypes of thymocytes, splenocytes, and bone marrow cells; and TREC levels were plotted as box/whisker plots, and differences in the median values across the indicated ages in the 2 mice strains were examined by Kruskall-Wallis ANOVA. Pairwise comparisons, for example, between genotype, between 2 age-groups, or control-vs.-treated cell cultures, were examined by *t* test, by post-hoc Tukey statistic or least square differences, or by Mann–Whitney *U* test, as appropriate. $P < 0.05$ was considered significant.

ACKNOWLEDGMENTS. We thank Cristina Iclozan and Sameem Abedin for contributions during the initial phase of the project; Mushtaq Ahmed for technical assistance; Megan Mason and Jacquelyn Grell for mouse husbandry and tissue collection; Dr. Greg Sempowski (Duke University) for TREC control reagents; Mayo Histology Core Laboratory for processing microscope slides; and Children's Hospital of Pittsburgh Imaging Lab for microscopy/automated imaging facilities. This work was supported by National Institutes of Health Grants R01 AG028141, R01 AG022379, R01 AI079047, and P20 CA103730; in part by the Mayo Foundation; and by the Department of Pediatrics, Children's Hospital of Pittsburgh, University of Pittsburgh.

1. Boldt HB, Conover CA (2007) Pregnancy-associated plasma protein-A (PAPP-A): A local regulator of IGF bioavailability through cleavage of IGFBPs. *Growth Horm IGF Res* 17:10–18.
2. Gyrup C, Oxvig C (2007) Quantitative analysis of insulin-like growth factor-modulated proteolysis of insulin-like growth factor binding protein-4 and -5 by pregnancy-associated plasma protein-A. *Biochemistry* 46:1972–1980.
3. Baker J, et al. (1993) Role of insulin-like growth factors in embryonic and postnatal growth. *Cell* 75:73–82.
4. Liu JP, et al. (1993) Mice carrying null mutations of the genes encoding insulin-like growth factor I (Igf-1) and type 1 IGF receptor (Igf1r). *Cell* 75:59–72.
5. Holzenberger M, et al. (2003) IGF-1 receptor regulates lifespan and resistance to oxidative stress in mice. *Nature* 42:182–187.
6. Mathews LS, et al. (1988) Growth enhancement of transgenic mice expressing human insulin-like growth factor I. *Endocrinology* 123:2827–2833.
7. van Buul-Offers SC, et al. (1995) Overexpression of human insulin-like growth factor-II in transgenic mice causes increased growth of the thymus. *J Endocrinol* 144:491–502.
8. O'Connor JC, et al. (2008) Regulation of IGF-I function by proinflammatory cytokines: At the interface of immunology and endocrinology. *Cell Immunol* 252:91–110.
9. Samani AA, Yakar S, LeRoith D, Brodt P (2007) The role of the IGF system in cancer growth and metastasis: Overview and recent insights. *Endocr Rev* 28:20–47.
10. Kenyon C (2005) The plasticity of aging: Insights from long-lived mutants. *Cell* 120:449–460.
11. Rincon M, Muzumdar R, Atzmon G, Barzilai N (2004) The paradox of the insulin/IGF-1 signaling pathway in longevity. *Mech Ageing Dev* 125:397–403.
12. Denley A, et al. (2005) Molecular interactions of the IGF system. *Cytokine Growth Factor Rev* 16:421–439.
13. Bartke A (2005) Role of the growth hormone/insulin-like growth factor system in mammalian aging. *Endocrinology* 146:3718–3723.
14. Yang J, Anzo M, Cohen P (2005) Control of aging and longevity by IGF-I signaling. *Exp Gerontol* 40:867–872.
15. Conover CA, et al. (2004) Metalloproteinase pregnancy-associated plasma protein A is a critical growth regulatory factor during fetal development. *Development* 131:1187–1194.
16. Conover CA, Bale LK (2007) Loss of pregnancy-associated plasma protein A extends lifespan in mice. *Aging Cell* 6:727–729.
17. Resch ZT, Simari RD, Conover CA (2006) Targeted disruption of the pregnancy-associated plasma protein-A gene is associated with diminished smooth muscle cell response to insulin-like growth factor-I and resistance to neointimal hyperplasia after vascular injury. *Endocrinology* 147:5634–5640.
18. Harrington SC, Simari RD, Conover CA (2007) Genetic deletion of pregnancy-associated plasma protein-A is associated with resistance to atherosclerotic lesion development in apolipoprotein E-deficient mice challenged with a high-fat diet. *Circ Res* 100:1696–1702.
19. Conover CA, Mason MA, Levine JA, Novak CM (2008) Metabolic consequences of pregnancy-associated plasma protein-A deficiency in mice: Exploring possible relationship to the longevity phenotype. *J Endocrinol* 198:599–605.
20. May RC (2007) Gender, immunity, and the regulation of longevity. *BioEssays* 29:795–802.
21. Vallejo AN (2007) Immune remodeling: Lessons from repertoire alterations during chronological aging and in immune-mediated disease. *Trends Mol Med* 13:94–102.
22. Mourkioti F, Rosenthal N (2005) IGF-1, inflammation and stem cells: Interactions during muscle regeneration. *Trends Immunol* 26:535–542.
23. Kecha O, et al. (1999) Characterization of the insulin-like growth factor axis in the human thymus. *J Neuroendocrinol* 11:435–440.
24. Montecino-Rodriguez E, Clark R, Dorshkind K (1998) Effects of insulin-like growth factor administration and bone marrow transplantation on thymopoiesis in aged mice. *Endocrinology* 139:4120–4126.
25. Taub DD, Longo DL (2005) Insights into thymic aging and regeneration. *Immunol Rev* 205:72–93.
26. Ciofani M, Zúñiga-Pflücker JC (2007) The thymus as an inductive site for T lymphopoiesis. *Annu Rev Cell Dev Biol* 23:463–493.
27. Sempowski GD, et al. (2002) T cell receptor excision circle assessment of thymopoiesis in aging mice. *Mol Immunol* 38:841–848.
28. Serwold T, et al. (2009) Reductive isolation from bone marrow and blood implicates common lymphoid progenitors as the major source of thymopoiesis. *Blood* 113:807–815.
29. Kecha O, et al. (2000) Involvement Involvement of insulin-like growth factors in early T cell development: A study using fetal thymic organ cultures. *Endocrinology* 141:1209–1217.
30. Kooijman R, et al. (1995) T cell development in insulin-like growth factor-II transgenic mice. *J Immunol* 154:5736–5745.
31. Zhou R, et al. (2004) Insulin-like growth factor-binding protein-4 inhibits growth of the thymus in transgenic mice. *J Mol Endocrinol* 32:349–364.
32. Ning Y, Schuller AG, Conover CA, Pintar JE (2008) Insulin-like growth factor (IGF) binding protein-4 is both a positive and negative regulator of IGF activity in vivo. *Mol Endocrinol* 22:1213–1225.
33. Graham DB, et al. (2006) CD28 ligation costimulates cell death but not maturation of double-positive thymocytes due to defective ERK MAPK signaling. *J Immunol* 177:6098–6107.
34. Yager EJ, et al. (2008) Age-associated decline in T cell repertoire diversity leads to holes in the repertoire and impaired immunity to influenza virus. *J Exp Med* 205:711–223.
35. Sadighi Akha AA, Miller RA (2005) Signal transduction in the aging immune system. *Curr Opin Immunol* 17:486–491.
36. Messaoudi I, et al. (2004) 17: Age-related CD8 T cell clonal expansions constrict CD8 T cell repertoire and have the potential to impair immune defense. *J Exp Med* 200:1347–1358.
37. Kruisbeek AM (2006) In vitro assays of lymphocyte function. In *Current Protocols in Immunology*, eds Coligan JE, et al. (John Wiley & Sons, NY).
38. Linton PJ, Dorshkind K (2004) Age-related changes in lymphocyte development and function. *Nat Immunol* 5:133–139.
39. Paula C, et al. (2009) Alterations in dendritic cell function in aged mice: Potential implications for immunotherapy design. *Biogerontology* 10:13–25.
40. Stout RD, Suttles J (2005) Immunosenescence and macrophage functional plasticity: Dysregulation of macrophage function by age-associated microenvironmental changes. *Immunol Rev* 205:60–71.
41. Verheijen R, et al. (1989) Ki67 detects a nuclear matrix-associated proliferation related antigen. II. Localisation in mitotic cells and association with chromosomes. *J Cell Sci* 92:531–540.
42. Kelley KW, Weigent DA, Kooijman R (2007) Protein hormones and immunity. *Brain Behav Immun* 21:384–392.
43. Lelbach A, Muzes G, Feher J (2005) The insulin-like growth factor system: IGFs, IGF-binding proteins, and IGFBP-proteases. *Acta Physiol Hung* 92:97–107.
44. Brocardo MG, et al. (2001) Early effects of insulin-like growth factor-1 in activated human T lymphocytes. *J Leukoc Biol* 70:297–305.
45. Bernabei P, et al. (2003) IGF-1 down-regulates IFN-gamma R2 chain surface expression and desensitizes IFN-gamma/STAT-1 signaling in human T lymphocytes. *Blood* 102:2933–2939.
46. Lemster BH, et al. (2008) Induction of CD56 and TCR-independent activation of T cells with aging. *J Immunol* 180:1979–1990.